

Supporting Information

Improving-Performance Photodetectors Based on MAPbBr₃ Film Optimization and MeOP-DSF Hole-Transport Layer

Ziyun Lin^a, Aocheng Jiang^a, Yujia Luo^a, Yuyao Feng^a, Yichi Zhang^a, Zeyao Han^b,
Wanling Mao^a, Yuhui Dong^{a,*}, Li Zhang^{b,*}, Yousheng Zou^{a,*}

^a MIIT Key Laboratory of Advanced Display Materials and Devices, Jiangsu Province Engineering Research Center of Quantum Dot Display, School of Materials Science and Engineering, Institute of Optoelectronics & Nanomaterials, Nanjing University of Science and Technology, Nanjing, Jiangsu 210094, China

^b State Key Laboratory of Organic Electronics and Information Displays, Institute of Advanced Materials (IAM), School of Material Science and Engineering, Nanjing University of Posts and Telecommunications (NUPT), Nanjing 210023, China

* Corresponding authors

E-mail: iamlizhang@njupt.edu.cn

dong.yuhui@njust.edu.cn

yshzou75@njust.edu.cn

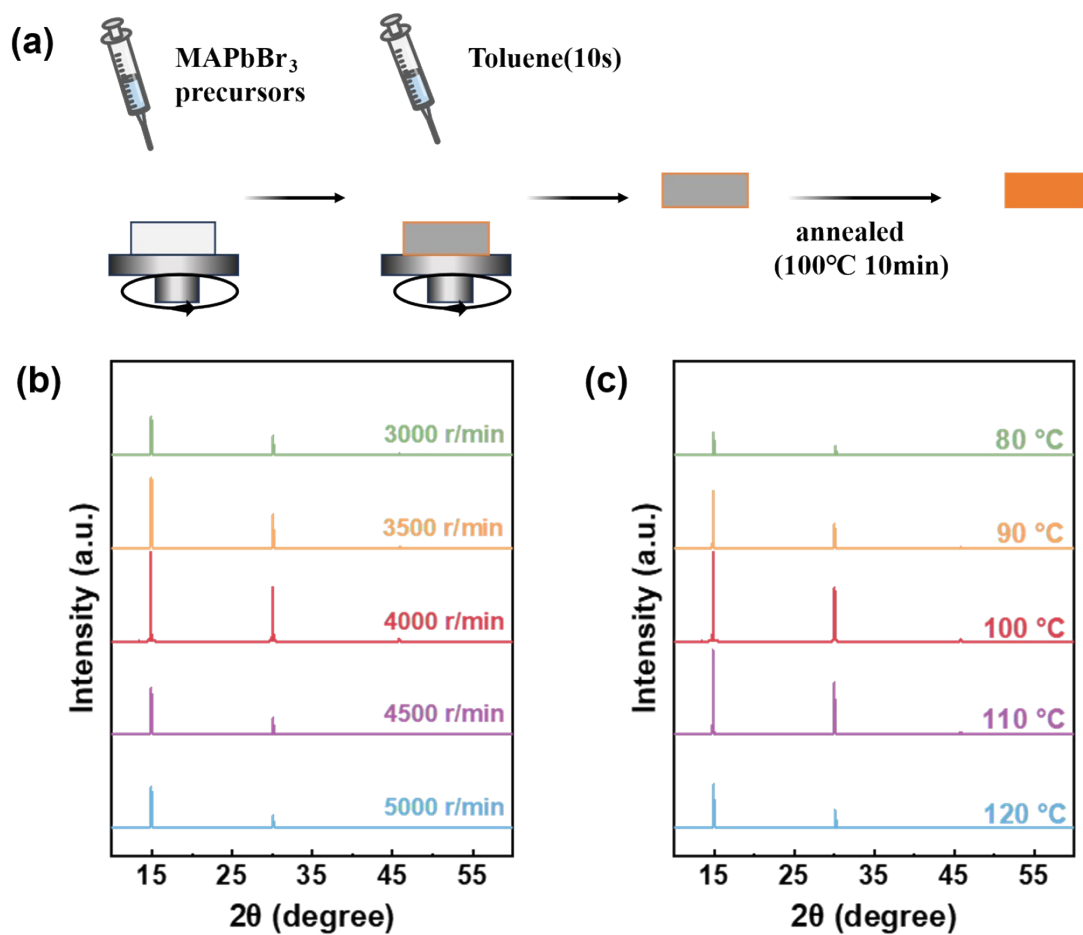


Fig. S1. (a) Preparation process of MAPbBr₃ film optimization; (b) XRD patterns of MAPbBr₃ films prepared at different spin-coating speeds and (c) different annealing temperatures.

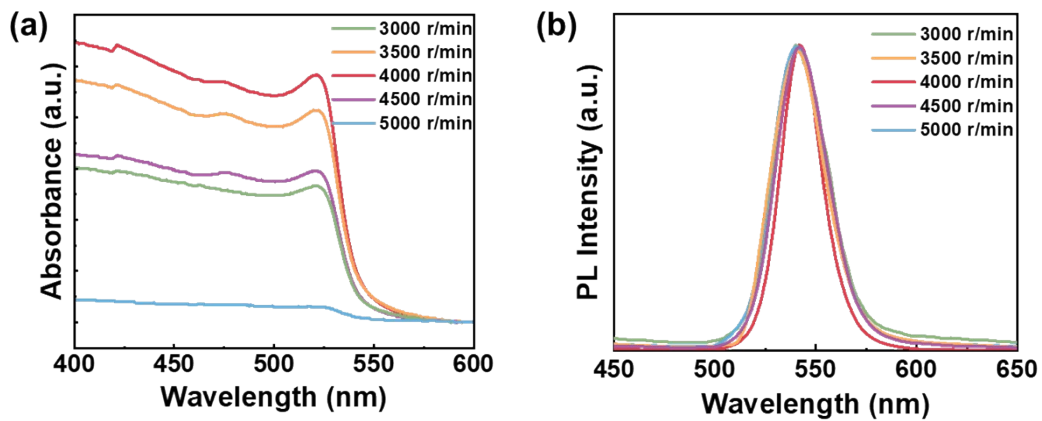


Fig. S2. (a) Absorption and (b) photoluminescence spectra of MAPbBr₃ films prepared at different spin-coating speeds.

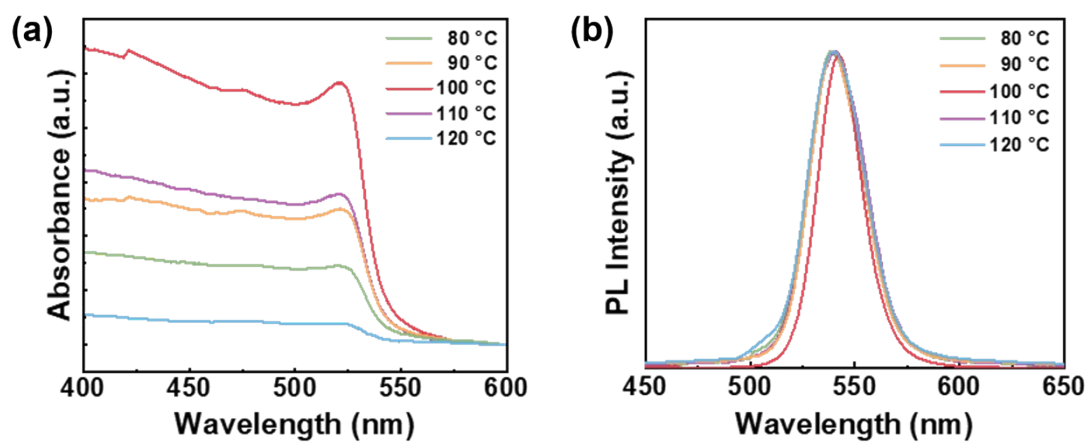


Fig. S3. (a) Absorption and (b) photoluminescence spectra of MAPbBr₃ films prepared at annealing different temperatures.

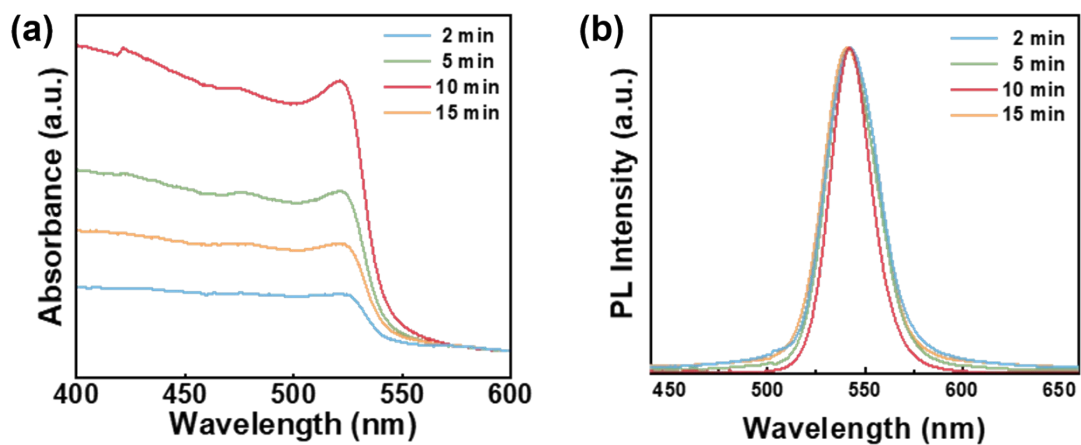


Fig. S4. (a) Absorption and (b) photoluminescence spectra of MAPbBr₃ films prepared with different annealing times.

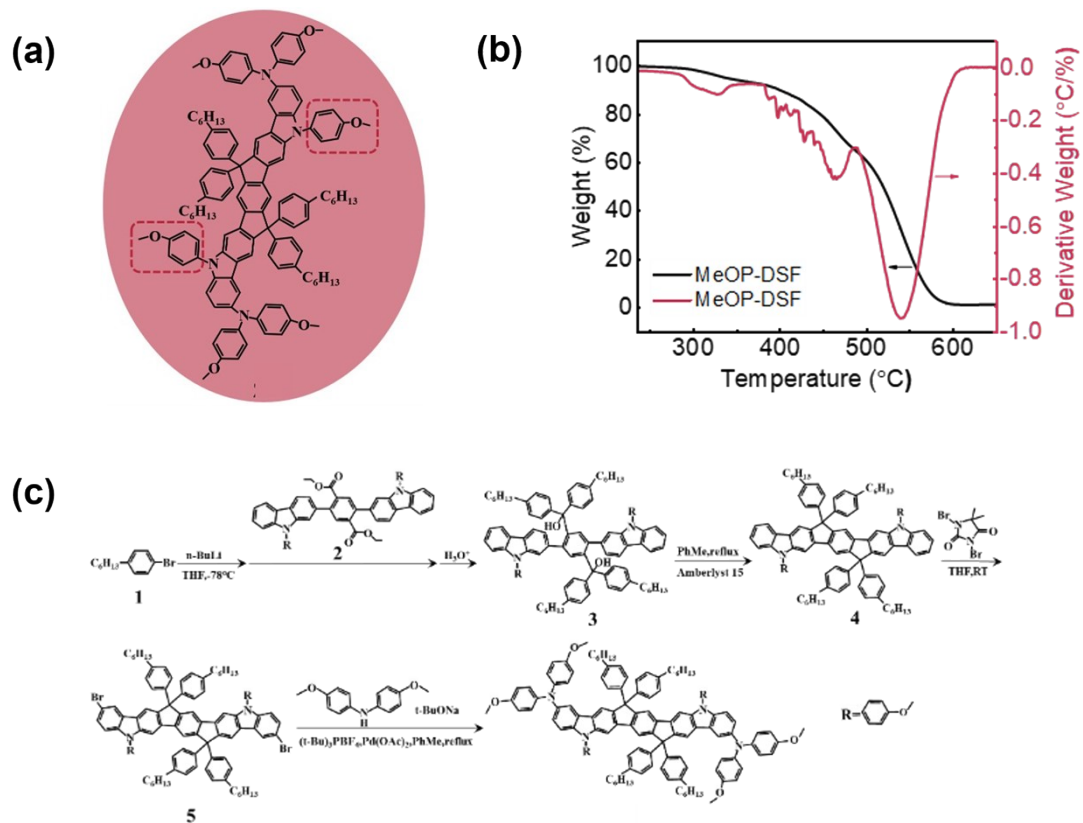


Fig. S5. (a) Schematic diagram of the structure of MeOP-DSF; (b) Thermogravimetric analysis (TGA) curve and (c) Schematic diagram of the synthesis process of the MeOP-DSF.

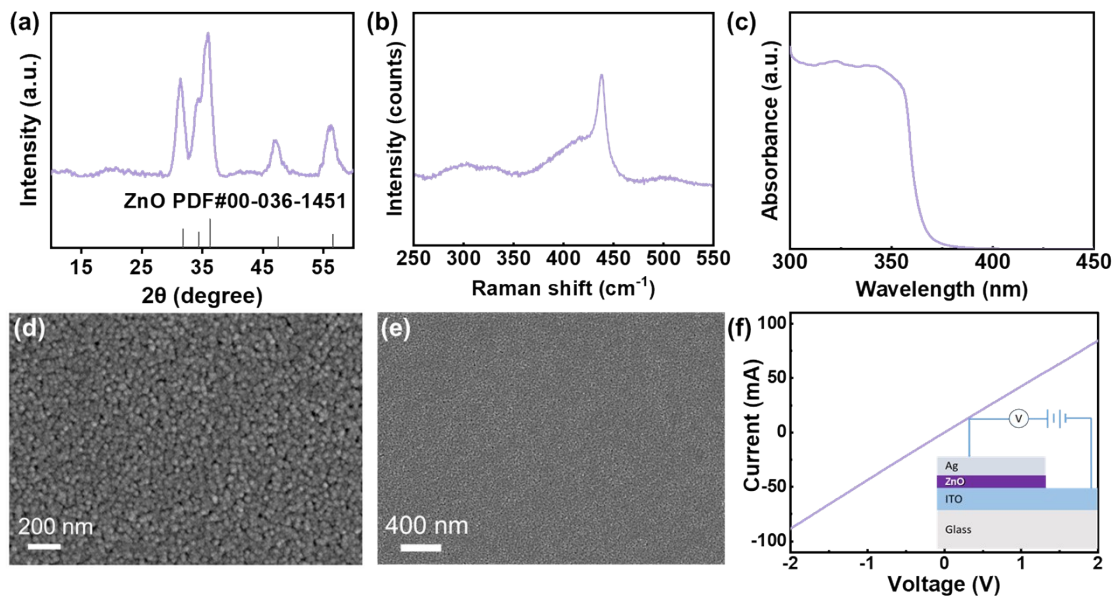


Fig. S6. (a) XRD pattern; (b) Raman spectrum; (c) Absorption spectrum; (d) SEM image; (e) High-magnification SEM image and (f) Current-voltage (I-V) curve of the as-assembled ZnO film.

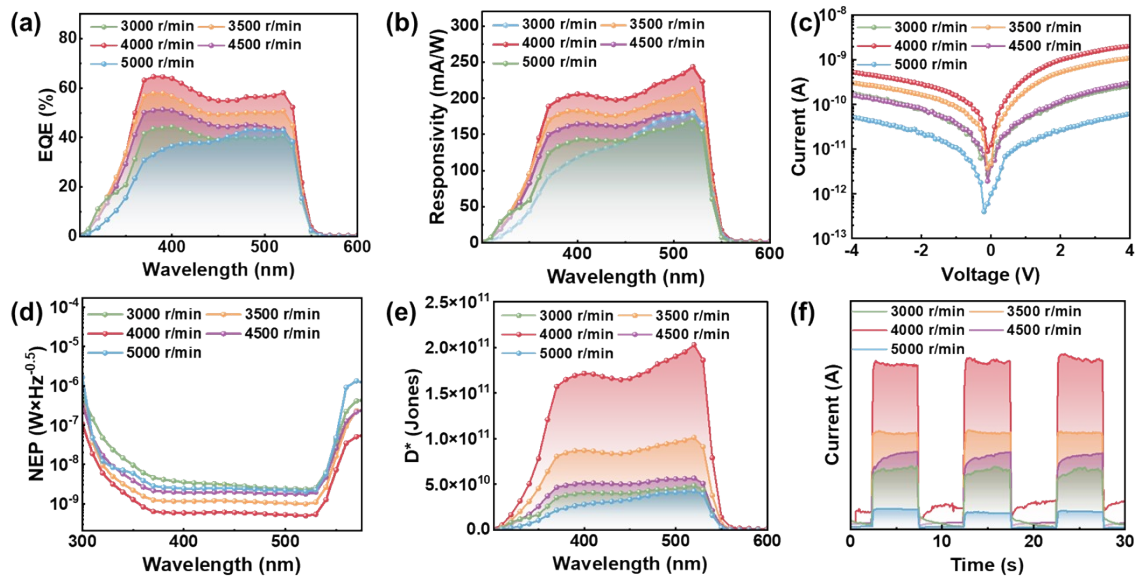


Fig. S7. (a) EQE; (b) Responsivity; (c) I-V curves under dark conditions; (d) Noise equivalent power (NEP); (e) Specific detectivity (D^*); (f) I-t curves of MAPbBr₃ devices fabricated at different spin-coating speeds.

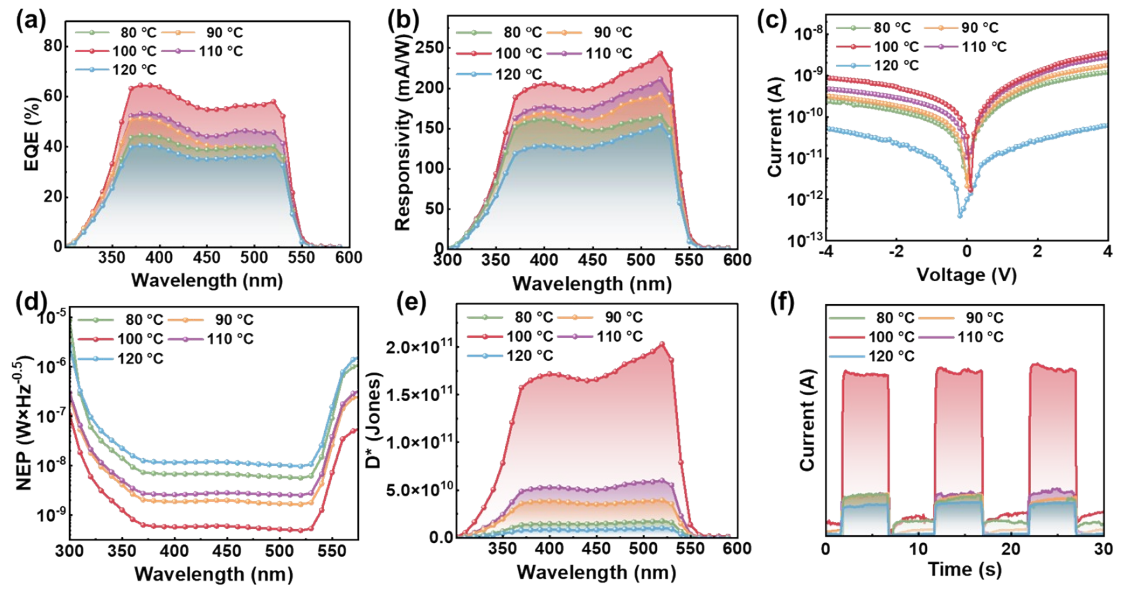


Fig. S8. (a) EQE; (b) Responsivity; (c) I-V curves under dark conditions; (d) Noise equivalent power (NEP); (e) Specific detectivity (D^*); (f) I-t curves of MAPbBr₃ devices fabricated at different annealing temperatures.

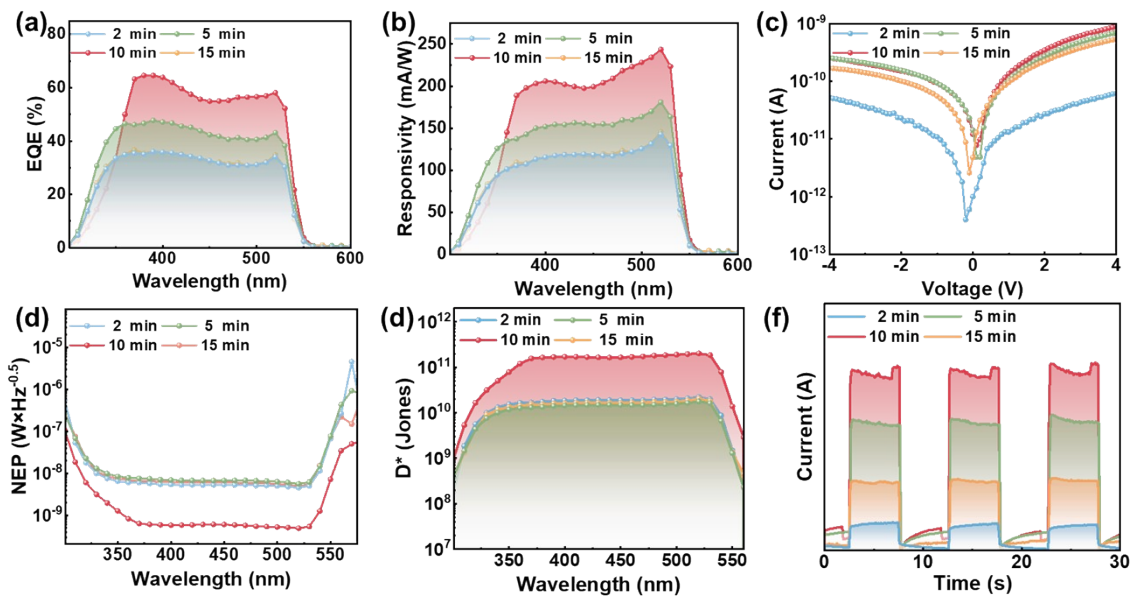


Fig. S9. (a) EQE; (b) Responsivity; (c) I-V curves under dark conditions; (d) Noise equivalent power (NEP); (e) Specific detectivity (D^*); (f) I-t curves of MAPbBr₃ devices fabricated at different annealing times.